

Noxa Up-regulation and Mcl-1 Cleavage Are Associated to Apoptosis Induction by Bortezomib in Multiple Myeloma

Patricia Gomez-Bougie,^{1,3} Soraya Wuillème-Toumi,^{1,2,3} Emmanuelle Ménoret,^{1,2,3} Valérie Trichet,^{2,4} Nelly Robillard,¹ Moreau Philippe,^{2,5} Régis Bataille,^{1,2,3} and Martine Amiot^{1,2,3}

¹Institut National de la Santé et de la Recherche Médicale, UMR601; ²Université de Nantes, Nantes Atlantique Universités, UFR Médecine et Techniques Médicales; ³Equipe 5 labélisée Ligue Nationale contre le Cancer 2005; ⁴Institut National de la Santé et de la Recherche Médicale ERI 7; ⁵Centre Hospitalier Universitaire, Service d'Hématologie Clinique, Nantes, France

Abstract

Targeting the ubiquitin-proteasome pathway has emerged as a potent anticancer strategy. Bortezomib, a specific proteasome inhibitor, has been approved for the treatment of relapsed or refractory multiple myeloma. Multiple myeloma cell survival is highly dependent on Mcl-1 antiapoptotic molecules. In a recent study, proteasome inhibitors induced Mcl-1 accumulation that slowed down their proapoptotic effects. Consequently, we investigated the role of Bcl-2 family members in bortezomib-induced apoptosis. We found that bortezomib induced apoptosis in five of seven human myeloma cell lines (HMCL). Bortezomib-induced apoptosis was associated with Mcl-1 cleavage regardless of Mcl-1L accumulation. Furthermore, RNA interference mediated Mcl-1 decrease and sensitized RPMI-8226 HMCL to bortezomib, highlighting the contribution of Mcl-1 in bortezomib-induced apoptosis. Interestingly, an important induction of Noxa was found in all sensitive HMCL both at protein and mRNA level. Concomitant to Mcl-1 cleavage and Noxa induction, we also found caspase-3, caspase-8, and caspase-9 activation. Under bortezomib treatment, Mcl-1L/Noxa complexes were highly increased, Mcl-1/Bak complexes were disrupted, and there was an accumulation of free Noxa. Finally, we observed a dissociation of Mcl-1/Bim complexes that may be due to a displacement of Bim induced by Noxa. Thus, in myeloma cells, the mechanistic basis for bortezomib sensitivity can be explained mainly by the model in which the sensitizer Noxa can displace Bim, a BH3-only activator, from Mcl-1, thus leading to Bax/Bak activation. [Cancer Res 2007;67(11):5418–24]

Introduction

The 26S proteasome is critical for the maintenance of homeostasis of most of intracellular proteins (1). A large number of proteins involved in cell cycle progression and apoptosis are regulated by ubiquitylation and proteasome-mediated degradation. Therefore, targeting proteasome pathway has emerged as a promising approach to cancer therapy (2). Bortezomib (PS341, Velcade, Millenium), a cell-permeable dipeptidyl boronic acid, is a specific and selective inhibitor of 26S proteasome. Bortezomib is the first proteasome inhibitor used for the treatment of relapsed or refractory multiple myeloma (3), an incurable disease characterized

by an accumulation of malignant long-lived plasma cells. Clinical trials comparing bortezomib with dexamethasone showed the superiority of bortezomib in terms of response rate and survival in patients with relapsed myeloma (3). Although bortezomib is able to bypass drug resistance and synergize with some conventional therapy, it was shown recently that bortezomib can trigger the accumulation of antiapoptotic factors responsible for a protective antitumor effect. This includes Mcl-1 antiapoptotic protein. Indeed, it was shown that the intrinsic cytotoxic activity of bortezomib is slowed down by the accumulation of Mcl-1 (4). Mcl-1 is particular among the antiapoptotic Bcl-2 members in that it is a short-lived protein that is rapidly induced and turned over (5). In multiple myeloma, the role of Mcl-1 can be distinguished from that of the other antiapoptotic members because we have found that only Mcl-1 antisenses trigger a rapid induction of apoptosis, which was observed neither with Bcl-2 nor with Bcl-x_L antisenses (6). Thus, Mcl-1 seems as one of the key proteins in regulating multiple myeloma cell survival. Both Mcl-1 mRNA and protein have a short half-life in multiple myeloma cells (7). In multiple myeloma cells, a large variety of stimuli (growth factor withdrawal, cytotoxic agents) induce the disappearance of Mcl-1 that is associated with the onset of apoptosis. In contrast, regardless of the apoptotic stimulus, Bcl-2 expression remains unchanged (8, 9). The disappearance of Mcl-1 can be explained by the combination of synthesis blockade, proteasome degradation, and/or proteolysis by caspases (5). We showed previously that Mcl-1 down-regulation is important to make multiple myeloma cells susceptible to BH3-only proteins and therefore to mitochondrial disruption (8). Until now, two different BH3-only have been involved in apoptosis induction by bortezomib (i.e., either the induction of the BH3-only protein Noxa or the accumulation of Bik/NBK; refs. 10–12). Because Mcl-1 is the essential survival protein in multiple myeloma and can be accumulated by bortezomib treatment, we examined its regulation and involvement in bortezomib-induced apoptosis. Short hairpin RNA (shRNA) technology was used in human myeloma cell lines (HMCL) to assess the specific role of Mcl-1 in response to bortezomib. The identification of the specific role of BH3-only proteins in apoptosis induction by bortezomib remains unclear. We found that Noxa contributes to apoptosis induction by bortezomib. Therefore, we were interested in the study of Noxa interactions to better understand its mechanism of action.

Materials and Methods

HMCL and culture conditions. The HMCL U266 and RPMI-8226 were purchased from DSM, and L363, LP1, and NCI-H929 were from the American Type Culture Collection. The interleukin-6 (IL-6)-dependent HMCL MDN has been established previously in our laboratory and is cultured in the presence of 3 ng/mL recombinant IL-6 (Novartis). KMS12PE was kindly provided by Dr. T. Ohtsuki (Kawasaki Medical School, Kurashiki,

Note: P. Gomez-Bougie and S. Wuillème-Toumi contributed equally to this work.
Requests for reprints: Martine Amiot, Institut National de la Santé et de la Recherche Médicale, U601, Département de recherche en Cancérologie, 9 quai Moncoussu, Nantes, F-44000 France. Phone: 33-2-40-08-47-66; Fax: 33-2-40-08-47-78; E-mail: mamiot@nantes.inserm.fr.

©2007 American Association for Cancer Research.
doi:10.1158/0008-5472.CAN-06-4322

Japan). Cells were maintained in RPMI 1640 supplemented with 5% FCS, 2 mmol/L glutamine, antibiotics (100 IU/mL penicillin and 100 µg/mL streptomycin), and 10 µmol/L 2-β-mercaptoethanol.

Antibodies (monoclonal antibodies) and reagents. Bortezomib was kindly provided by Millenium Pharmaceuticals, Inc. Anti-Mcl-1 monoclonal antibody (mAb; clone RC 13) and anti-Bcl-2 (clone 124) mouse mAbs were obtained from Neomarkers (Interchim) and DAKO, respectively. Antibodies against caspase-3 (mouse mAb), caspase-9 (F7 mouse mAb), Bik (goat polyclonal), and Mcl-1 (S19, rabbit polyclonal) were from Santa Cruz Biotechnology (Tebu-Bio) and caspase-8 from Cell Signaling Technology. Antibodies against Noxa and Bak (TC-100) were from Alexis and Oncogene, respectively. Anti-F1-ATPase and anti-Bim rabbit polyclonal antibodies were obtained from Molecular Probes and Calbiochem, respectively. Immobilized recombinant protein A-Sepharose was obtained from Interchim and zVAD-fmk was from Promega.

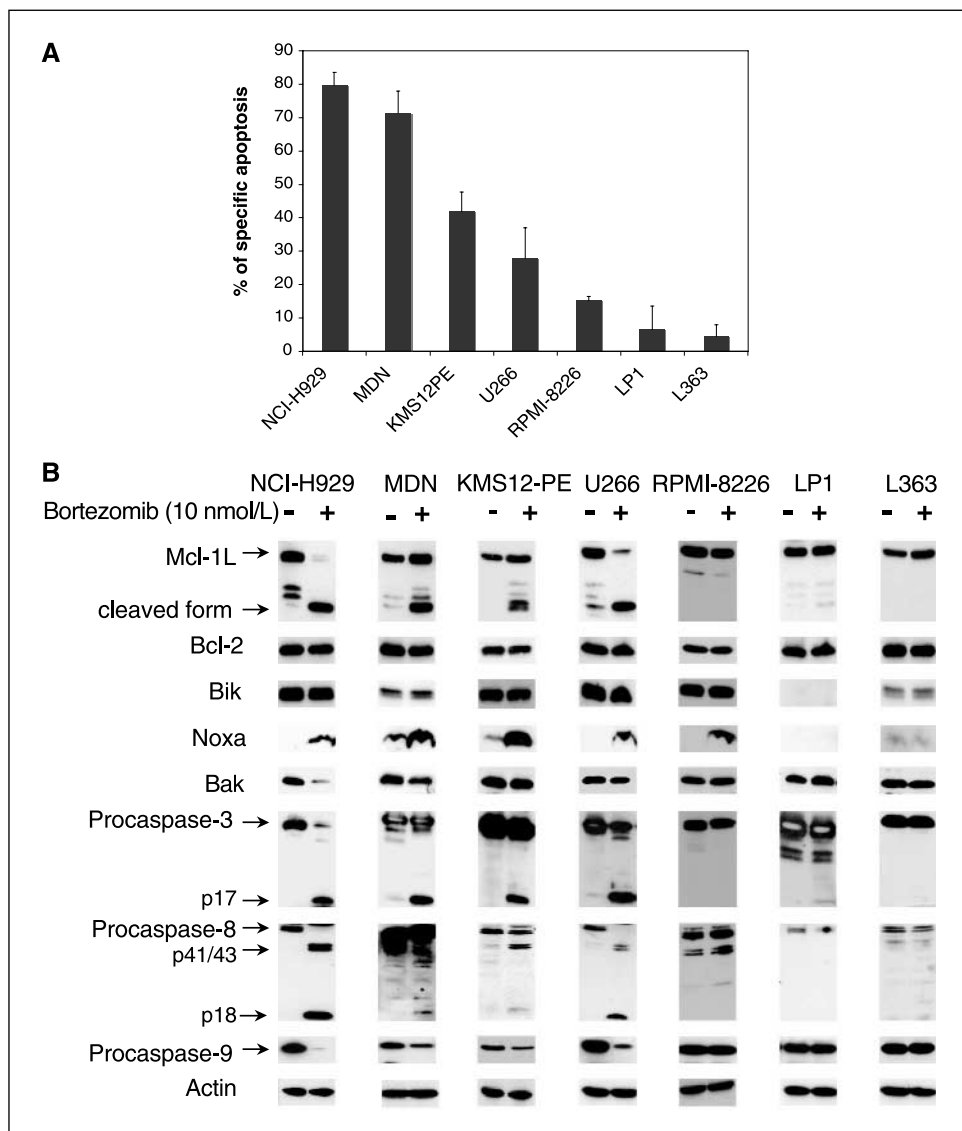
Lentiviral vector construction for RNA interference. Two lentiviral vectors, pLenti-CD90-sh-Mcl-1 and pLenti-CD90-sh-Luci, were generated as described previously (13) to produce shRNA directed against human Mcl-1 (accession no. NM-021960) or firefly luciferase mRNA, respectively. Briefly, they were derived from the pLenti6/V5-GW/LacZ plasmid (Invitrogen Corp.), whose *LacZ* and *blastidicin* genes have been replaced by a marker gene coding for CD90 membrane protein. In addition, they contain a genomic cassette composed of H1 promoter plus sequence for shRNA

synthesis. Mcl-1 shRNA was designed to target the following *Mcl-1* gene sequence (ACGCGGTAATCGACTCAA).

Virus production and cell transduction. Viral productions were done following the guidelines of the ViraPower Lentiviral Expression System (Invitrogen). Briefly, 3×10^6 293FT cells were transfected using the calcium phosphate method with 9 µg of the optimized packaging mix and 3 µg pLenti-CD90-shRNA. Virus-containing supernatants were harvested 48 h after transfection and concentrated by ultracentrifugation. For titration, serial dilutions of viral production were tested on 293FT cells that were analyzed for CD90 expression by fluorescence-activated cell sorting (FACS) 72 h after infection. We usually obtained titers ranging from 5×10^6 to 5×10^7 viral units/mL. To generate stably modified RPMI-8226 cell lines, 10^5 cells were placed in 200 µL of medium within a well of 24-well plate and infected at a multiplicity of 8 with either Lenti-CD90-sh-Mcl-1 or Lenti-CD90-sh-Luci viral units. Ten days after infection, 80% of transduced RPMI-8226 cells were identified by their overexpression of CD90 and sorted out using FACS analysis. By this approach, we obtained a control population, named shLuci-RPMI-8226 and another one, named shMcl-1-RPMI-8226.

Noxa RNA interference assay. The small interfering RNA (siRNA) used to silence *Noxa* gene (*Noxa* siRNA) was N8 5'-GUAUUUUUGACACAUUU-CUU-3' (14). Both siRNA and Silencer^R Negative Control siRNA (AM4635) were synthesized by Ambion. U266 cell line was electroporated using a Nucleofector system (Amamax) according to the manufacturer's instructions.

Figure 1. Bortezomib induced cleavage of Mcl-1, Noxa induction, and activation of caspases in sensitive myeloma cells. **A**, HMCL are differentially sensitive to bortezomib. HMCL (125,000 cells/0.25 mL in 96-well plate) were treated for 24 h with 10 nmol/L bortezomib. Cells were stained with APO2.7-phycoerythrin (PE) and analyzed with a FACSCalibur. **B**, HMCL were treated for 24 h with 10 nmol/L bortezomib. Cell lysates were separated by SDS-PAGE and then electrotransferred onto PVDF membranes. The membranes were probed with the respective antibodies. Actin was included as a protein loading control.



Briefly, 5×10^6 U266 cells were resuspended in 100 μ L R nucleofector solution containing 10 μ mol/L siRNA and electroporated with T01 Nucleofector program. Cells were transferred to culture plates and cultured at 5×10^5 cells/mL for 2 h before incubation with bortezomib.

Assay for detection of apoptotic cells. Cell death was assessed by APO2.7 (Beckman Coulter) staining according to the manufacturer's recommendation. Flow cytometry analysis was done on a FACSCalibur using the CellQuest software (Becton Dickinson).

Caspase activity. Caspase activity was detected as described previously (15). Briefly, cell lysates were prepared as described for immunoblotting. Caspase activity was measured by following the cleavage of 50 μ mol/L peptide Ac-DEVD-AMC (caspase-3), Ac-IETD-AMC (caspase-8), or Ac-LEHD-AMC (caspase-9), respectively. The fluorescence of the cleaved substrate was determined every 15 min using a spectrophotometer (Fluorolite 1000, Dynatech Laboratories) set at an excitation wavelength of 365 nm and emission wavelength of 465 nm. Fluorogenic peptides Ac-DEVD-AMC, Ac-IETD-AMC, and Ac-LEHD-AMC were purchased from Bachem.

Immunoblotting. Cells (5×10^6) were resuspended in lysis buffer [10 mmol/L Tris (pH 7.6), 150 mmol/L NaCl, 5 mmol/L EDTA, 1% Triton X-100] containing protease inhibitors. After 40 min on ice, lysates were cleared by centrifugation at $12,000 \times g$ for 30 min at 4°C . Protein concentrations were determined using bicinchoninic acid protein assay (Pierce). Equal amounts of total protein (70 mg/lane) were separated by SDS-PAGE, transferred onto polyvinylidene difluoride (PVDF) membranes, and analyzed following standard procedures. The signal was detected by enhanced chemiluminescence detection (Pierce).

Immunoprecipitation. Cells (25×10^6) were lysed in 1% CHAPS-containing lysis buffer. Whole-cell lysates were obtained, precleared with Protein A-Sepharose, and incubated overnight with 5 μ g of the specific antibody. The immunocomplexes were captured with protein A. Beads were pelleted, washed thrice, and boiled in SDS sample buffer. The presence of immunocomplexes was determined by Western blotting analysis.

Subcellular fractionation. Subcellular fractionation was adapted from a published protocol (16). Cells were washed once with ice-cold PBS and incubated in hypotonic buffer [5 mmol/L HEPES (pH 7.4), 0.025 mol/L sucrose, 2 mmol/L EDTA, 2 μ mol/L aprotinin, 0.4 mmol/L pefabloc] for 30 min on ice. Cells were disrupted with a dounce homogenizer, sucrose was added to 250 mmol/L and centrifuged at $500 \times g$ for 10 min to recover the nuclear pellet. The collected supernatant was centrifuged at $10,000 \times g$ for 15 min to obtain the heavy membrane pellet. The supernatant was collected as the cytoplasmic fraction. Heavy pellets were lysed in lysis buffer. Nuclear pellets were washed once in hypotonic buffer, sonicated in lysis buffer, and cleared by centrifugation at $12,000 \times g$ for 30 min at 4°C .

Quantitative real-time reverse transcription-PCR. One microgram of the total RNA was reverse transcribed using the Maloney murine leukemia virus reverse transcriptase (Invitrogen) and random hexamers (Amersham). Quantitative PCR was done using the Brilliant SYBR Green QPCR Core reagent kit and the MX4000 instrument (Stratagene) according to the manufacturer's instructions. The thermal cycling variables used were as follows: 40 cycles at 95°C for 30 s, 60°C for 30 s, and 72°C for 30 s. To control specificity of the amplified product, a melting curve analysis was done. No amplification of unspecific product was observed. Amplification of cyclophilin was carried out for each sample as endogenous control. Primer sequences were 5'-GCTGGAAGTCGAGTGTGCTA-3' (forward) and 5'-CCT-GAGCAGAAGAGTTTGA-3' (reverse) for Noxa and 5'-CCCACCGTGTCTT-CGACAT-3' (forward) and 5'-CCAGTGCTCAGAGCACGAAA-3' (reverse) for cyclophilin. The relative expression ratio of the Noxa gene was calculated according to the equation of Pfaffl (17) using untreated cells as reference.

Results

Bortezomib triggers Mcl-1 cleavage, Noxa induction, and caspase activation in sensitive HMCL. The ability of bortezomib to induce apoptosis was evaluated in seven HMCL by APO2.7 staining after 24 h of 10 nmol/L bortezomib treatment, which is in the range of therapeutic concentrations. Five of seven HMCL were

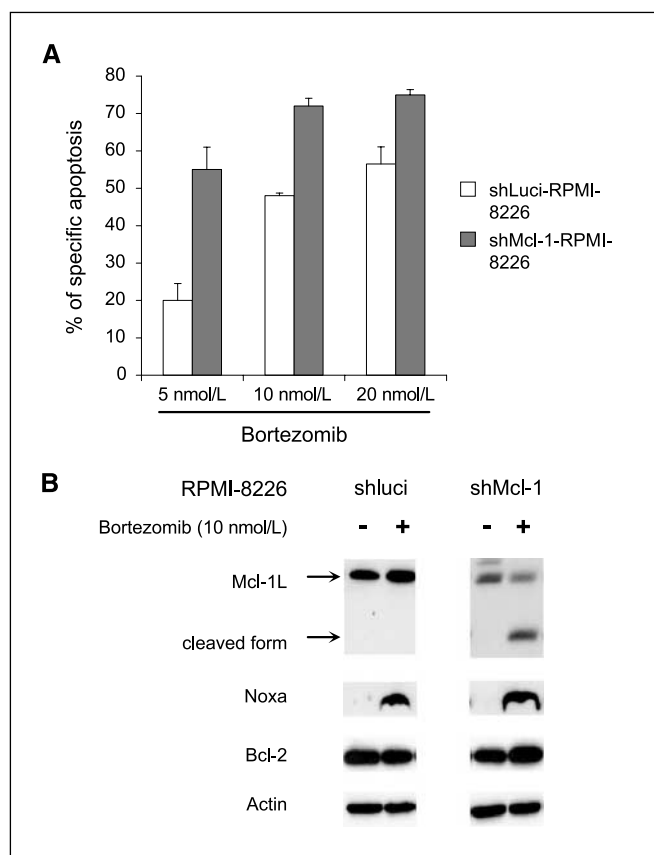


Figure 2. Mcl-1 down-regulation sensitizes RPMI-8226 cells to bortezomib. **A**, cells were treated 48 h by 5, 10, or 20 nmol/L bortezomib, stained with APO2.7-PE, and analyzed with a FACSCalibur. **B**, shLuci-RPMI-8226 and shMcl-1-RPMI-8226 cells were treated 24 h by 10 nmol/L bortezomib. An equivalent of 70 μ g protein per lane was separated by SDS-PAGE and then electrotransferred onto PVDF membranes. The membranes were probed with the respective antibodies.

sensitive to bortezomib (Fig. 1A). We observed that HMCL are differentially sensitive to bortezomib; we found very sensitive HMCL ($\geq 40\%$ of apoptotic cells), intermediate sensitive HMCL ($>25\%$ and $<40\%$ of apoptotic cells), and weakly sensitive HMCL ($<25\%$ of apoptotic cells).

Several members of the Bcl-2 family are known targets of bortezomib; thus, we studied the effect of 24 h of bortezomib treatment on antiapoptotic (Mcl-1 and Bcl-2) and proapoptotic (Noxa, Bik, and Bak) protein expression. Previous reports showed that bortezomib exposure leads to Mcl-1L accumulation (10, 11). In our study, all sensitive HMCL displayed Mcl-1 modifications at the expression level. Indeed, bortezomib treatment induced either a down-regulation (NCI-H929, U266, and RPMI-8226) or an accumulation (MDN and KMS-12-PE) of Mcl-1L. Strikingly, despite the modification of Mcl-1L level induced by bortezomib, we detected a cleavage of Mcl-1 as a general feature of highly sensitive HMCL (Fig. 1B). In contrast, no Mcl-1 cleavage was observed in the weakly sensitive RPMI-8226 or resistant LP1 and L363 HMCL. Bcl-2 levels were not substantially affected under bortezomib exposure. Of interest, Noxa BH3-only protein was strongly induced in all sensitive HMCL but it was not detected in LP1 or L363. Bik levels were not modified in any HMCL, suggesting that this BH3-only protein is not responsible for bortezomib-induced apoptosis. Finally, although Bak levels were not consistently affected in all sensitive HMCL, a down-regulation was often observed. Thus,

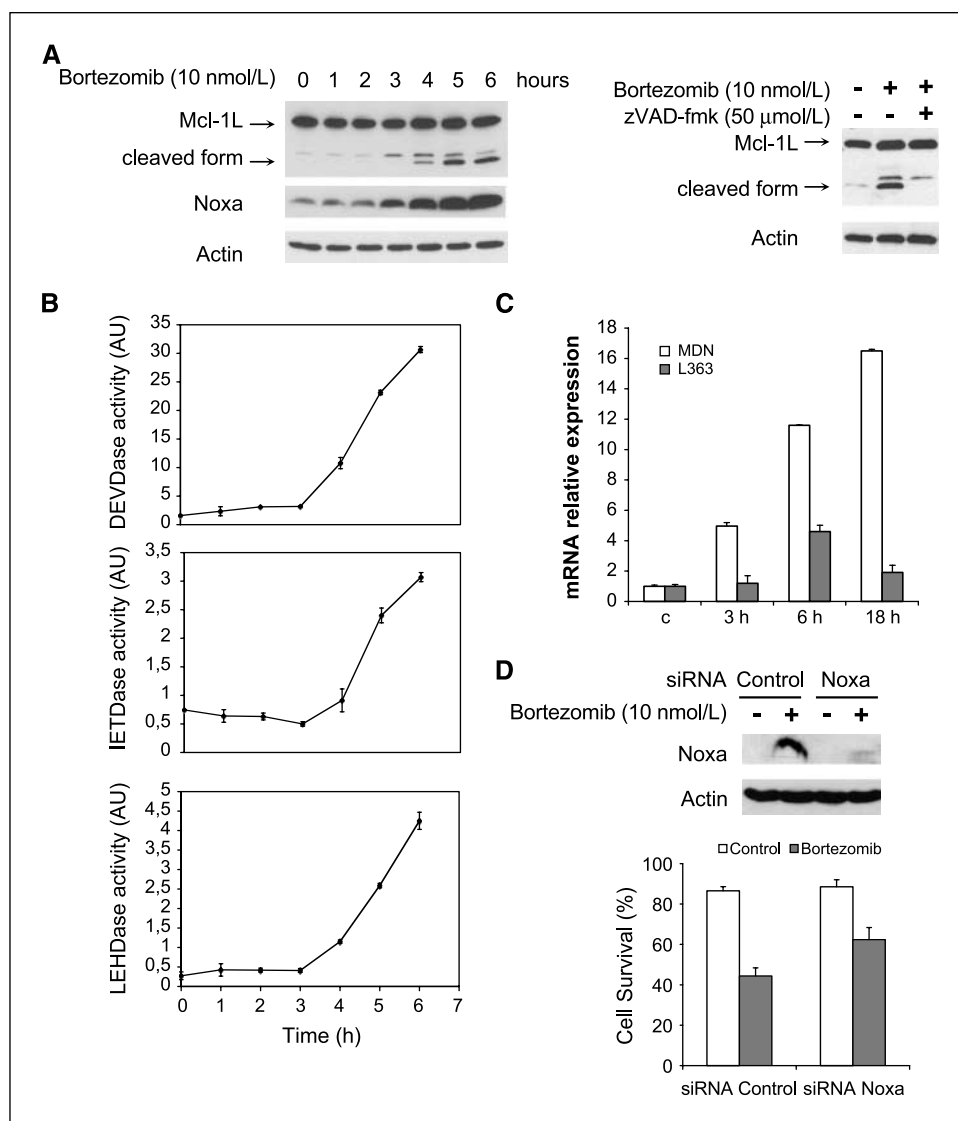
Mcl-1 cleavage and a significant Noxa induction are crucial events of bortezomib-induced apoptosis. To characterize the apoptotic machinery mediating bortezomib-induced apoptosis, we next investigated the activation (as detected by cleavage) of the initiators caspase-8 and caspase-9 as well as of the downstream effector caspase-3 (Fig. 1B). Activation of caspase-8, caspase-9, and caspase-3 was observed in highly sensitive cell lines after 24 h of bortezomib treatment. By contrast, the weakly sensitive RPMI-8226 and the resistant LP1 and L363 HMCL did not exhibit caspase activation.

Mcl-1 down-regulation sensitizes RPMI-8226 cells to apoptosis induction by bortezomib. To definitively establish the role of Mcl-1 in bortezomib-induced apoptosis in myeloma cells, we made use of RNA interference (RNAi) technology. We infected RPMI-8226 cells with lentivirus for the delivery of shRNA directed against Mcl-1 mRNA. shLuci-RPMI cells were generated to evaluate the potential effects caused by siRNA synthesis and distinguished them from the specific effects due to Mcl-1 down-regulation. Immunoblot analysis of Mcl-1 showed that shMcl-1-RPMI-8226 cells were characterized by a down-regulation of Mcl-1 corresponding to 50% reduction compared with shLuci-RPMI-8226 cell

population (Fig. 2B). Only a partial down-regulation of Mcl-1 allowed us to obtain viable Mcl-1 silencing RPMI-8226 cells because Mcl-1 is the essential survival protein for multiple myeloma cells. Mcl-1 knockdown sensitized RPMI-8226 cells to bortezomib-induced apoptosis as detected by 35%, 24%, and 18% increase of apoptotic cells at 5, 10, and 20 nmol/L, respectively (Fig. 2A). Moreover, when both shMcl-1-RPMI-8226 and shLuci-RPMI-8226 cells were treated by bortezomib for 24 h, the most significant difference was the cleavage of Mcl-1 (Fig. 2B). This cleavage was only observed in shMcl-1-RPMI-8226.

Noxa induction is essential for bortezomib-induced apoptosis. We did a kinetic analysis in MDN cells to characterize the implication of Mcl-1 and Noxa in bortezomib-induced apoptosis. The cleavage of Mcl-1 and the increase of Noxa levels were both early events in apoptosis induction. Mcl-1 cleavage was caspase dependent because preincubation with pan-caspase inhibitor zVAD-fmk totally prevented the generation of the cleaved form (Fig. 3A). Moreover, measurement of caspase activity (caspase-3, caspase-8, and caspase-9) showed caspases activation as early as 4 h of treatment concomitantly to Mcl-1 cleavage (Fig. 3B). To evaluate whether the increase of Noxa was due to an induction of

Figure 3. Mcl-1 cleavage, Noxa induction, and caspase activation are early events of bortezomib-induced cell death. **A**, MDN cell line was treated with 10 nmol/L bortezomib for the indicated times or incubated with 50 mmol/L ZVAD-fmk for 1 h followed by 10 nmol/L bortezomib for 6 h. Cell lysates were subjected to Western blotting analysis. Membranes were probed with the respective antibodies. **B**, caspase activity was measured on cell lysates using 50 μmol/L Ac-DEVD-AMC (caspase-3), Ac-IETD-AMC (caspase-8), or Ac-LEHD-AMC (caspase-9), respectively. Results were expressed in arbitrary units (AU). Points, mean of three different determinations. **C**, MDN and L363 cell lines were treated with 10 nmol/L bortezomib over 3, 6, and 18 h. Noxa mRNA levels were evaluated at these time points by quantitative reverse transcription-PCR. Noxa mRNA levels are given in relative expression ratio using untreated cells as reference and *cyclophilin* as housekeeping gene. **D**, knockdown of Noxa using siRNA decreases bortezomib-induced apoptosis. U266 cells were transfected with Noxa siRNA or control siRNA, 2 h after transfection, cells were treated with 10 nmol/L bortezomib for 24 h, and cell lysates were probed with anti-Noxa mAb. After 72 h of bortezomib treatment, cell viability was determined by trypan blue exclusion assay. Columns, mean of four independent experiments; bars, SD.



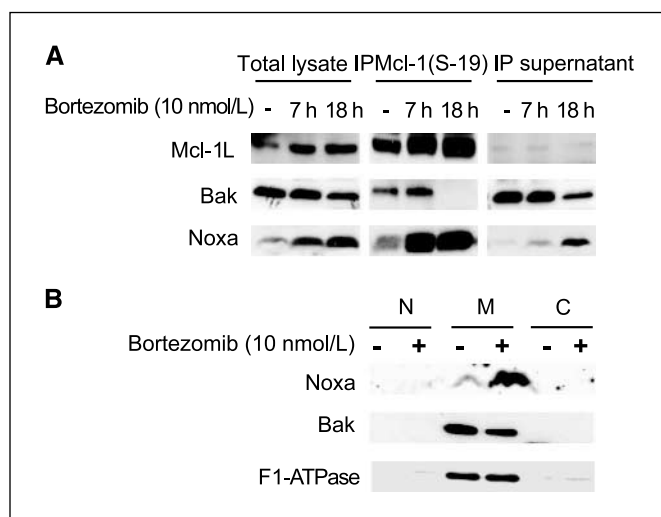


Figure 4. Disruption of Mcl-1/Bak complex and accumulation of free Noxa are hallmark of cell death induced by bortezomib. **A**, MDN cells were treated as indicated and immunoprecipitations (IP; 1 mg cell lysate) were carried out with 5 μ g rabbit polyclonal anti-Mcl-1 antibody. The presence of immunocomplexes was determined by Western blotting analysis, 5% of total lysates, and immunoprecipitation supernatants were also analyzed. **B**, bortezomib-induced Noxa is exclusively localized in mitochondria. After 7 h of bortezomib treatment, cells were subjected to subcellular fractionation as described (16). Nuclear (N), mitochondrial (M), and cytoplasmic (C) fractions were subjected to Western blotting analysis and membranes were probed with the specific antibodies. F1-ATPase was included as mitochondria marker.

transcription, we did quantitative, real-time PCR analysis. Eighteen hours of bortezomib treatment triggered a 15-fold increase in Noxa mRNA levels in MDN-sensitive HMCL, whereas it had no effect in L363-resistant HMCL (Fig. 3C). This result suggests that transcription of Noxa plays an important role in Noxa up-regulation. To determine whether Noxa played an essential role in bortezomib-induced apoptosis, we used siRNA to knock down Noxa expression. Noxa siRNA inhibited the induction of Noxa by bortezomib (Fig. 3D). The knockdown of Noxa provided protection against bortezomib-mediated apoptosis in U266 HMCL (Fig. 3D).

Disruption of Mcl-1/Bak complex and accumulation of free Noxa. It has been proposed that Mcl-1L forms constitutive complexes with proapoptotic Bak that are disrupted in apoptotic cells. To induce apoptosis, Bak should be released from Mcl-1 complex, probably displaced by Noxa (18). To address this mechanism in multiple myeloma cells, we analyzed the endogenous complexes between the antiapoptotic and the proapoptotic members and their modifications under bortezomib treatment. We first confirmed that Mcl-1L was constitutively associated to Bak (Fig. 4A). For the first time, we showed the presence of endogenous Mcl-1L/Noxa complexes in MDN cells that express a weak endogenous Noxa level. This result was expected because Noxa displays a high specificity for Mcl-1L (19). After 7 h of bortezomib treatment, we observed an increase of both Mcl-1L/Bak and Mcl-1L/Noxa complexes. The Mcl-1L/Bak complexes became undetectable after 18 h (Fig. 4A). This may be due to the disruption of the Mcl-1L/Bak complex. However, the combined analysis of both total lysates and immunoprecipitation supernatants together with the coimmunoprecipitation products suggests that the decrease of Mcl-1L/Bak complex could be also explained by the decrease of Bak induced by bortezomib treatment. Moreover, subcellular fractionation into nuclear, mitochondrial, and cytoplasmic fractions showed that the decrease of Bak level was also evident at the

mitochondria (Fig. 4B). It is worth noting that, despite the high level of Mcl-1/Noxa interaction under bortezomib treatment, free Noxa was detected in its respective immunoprecipitation supernatants (Fig. 4A). We also showed that Noxa is exclusively located in the mitochondrial fraction either constitutive or accumulated under bortezomib treatment (Fig. 4B). Thus, we can hypothesize that free Noxa may induce, directly or indirectly, mitochondria dysfunction.

Noxa induction could result in disruption of Mcl-1/Bim complexes. Because we reported previously the relevance of the disruption of Mcl-1/Bim complexes in myeloma cells undergoing apoptosis (8, 9), we assessed the modification of these complexes under bortezomib treatment. Endogenous Mcl-1/Bim and Bcl-2/Bim complexes were abundantly found in healthy MDN HMCL. After 7 h of bortezomib treatment, Mcl-1/Bim complexes were barely detectable, whereas the Bcl-2/Bim complexes were not modified (Fig. 5). Although, analysis of total lysates showed no modification of Bim levels and an accumulation of Mcl-1, Bim immunoprecipitates revealed the disruption of Mcl-1/Bim complexes as observed by the absence of Mcl-1 associated to Bim (Fig. 5). Because Noxa displays very high specificity for Mcl-1 and was abundantly induced in MDN cells after bortezomib treatment, we can hypothesized that Noxa displaces Bim from Mcl-1 as suggested by the appearance of abundant Mcl-1/Noxa complexes (Fig. 4A). Bim release may therefore trigger mitochondria dysfunction. A model by which the interplay between these Bcl-2 subfamily members determines cell death under bortezomib treatment is provided in Fig. 6.

Discussion

Proteasome inhibitors represent a novel class of compounds with promising antitumor activity. The clinical efficacy of the proteasome inhibitor bortezomib has been shown in the treatment of patients with refractory and relapsed multiple myeloma and other tumors (20). In this report, we show that bortezomib, at the pharmacologic concentration of 10 nmol/L, triggers apoptosis in five of seven HMCL, allowing to define sensitive and resistant HMCL. Although effective as an antitumor target, proteasome inhibition was implicated in the accumulation of the antiapoptotic protein Mcl-1L (4), whose elimination has been proposed to be required for apoptosis induction by different stimuli (8, 21). In our study, regardless to the decrease or the accumulation of Mcl-1L

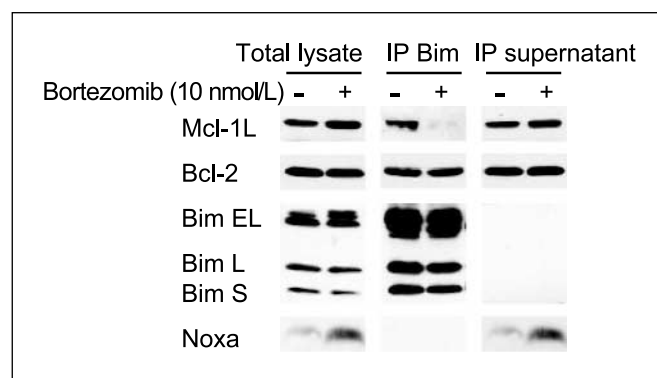
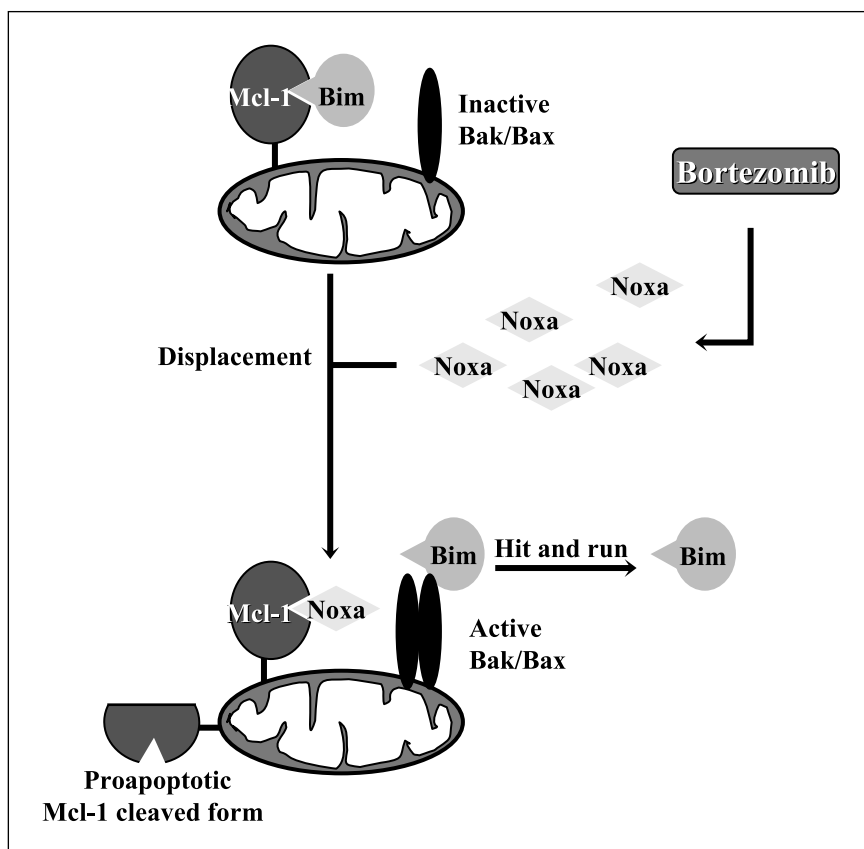


Figure 5. Early disruption of Bim/Mcl-1 complex under bortezomib treatment. MDN cells were treated during 7 h with 10 nmol/L bortezomib. Immunoprecipitations (1 mg cell lysate) were carried out with 5 μ g anti-Bim rabbit polyclonal antibody. The presence of immunocomplexes was determined by Western blotting analysis, 5% of total lysates, and immunoprecipitation supernatants were also analyzed.

Figure 6. Model of the interplay between antiapoptotic and proapoptotic molecules of the Bcl-2 family under bortezomib treatment. In myeloma cells, Mcl-1 protein sequesters the “direct activator” BH3-only Bim. Under bortezomib treatment, induction of the “sensitizer” BH3-only Noxa allows the displacement of the “direct activator” Bim, which is now able to activate Bax/Bak by a “hit and run” mechanism, triggering mitochondrial dysfunction and apoptosis.



induced by bortezomib in responsive HMCL, the cleavage of Mcl-1 was a hallmark of bortezomib sensitivity. Because the deregulation of antiapoptotic factors by bortezomib could negatively affect its antitumor effect (4), we explored the implication of Mcl-1 by RNAi in HMCL. shMcl-1-RPMI-8226 were more sensitive to bortezomib than shLuci-RPMI-8226. This result underscores the contribution of Mcl-1 to bortezomib apoptosis induction. It is worth noting that bortezomib increased sensitivity in shMcl-1 RPMI-8226 is associated with the generation of a cleaved Mcl-1 form, confirming its relevance in bortezomib-induced apoptosis. Kinetic studies indicated that Mcl-1 cleavage was detected as soon as caspases were activated. Moreover, pan-caspase inhibitor zVAD-fmk completely prevented the appearance of the cleaved form, confirming the direct involvement of caspase-3 and caspase-8 in Mcl-1 cleavage (22). Consequently, Mcl-1 cleavage occurs following apoptosis commitment. It has been shown recently that Mcl-1 cleavage products have a proapoptotic function (5); therefore, their induction under bortezomib treatment could amplify the apoptotic cascade. Of interest, apoptosis in all sensitive HMCL was consistently accompanied by the strong induction of the BH3-only protein Noxa. In contrast, we did not find an up-regulation of the BH3-only protein Bik, implicated previously in proteasome-mediated apoptosis (12). Our results point out that both, the level of Noxa induction and the cleavage of Mcl-1, clearly contribute to bortezomib-induced apoptosis. Our results agree with Qin et al. (10, 23) that showed bortezomib-induced apoptosis of melanoma cells was associated with Noxa induction. Furthermore, Noxa knockdown experiments confirmed the important role of Noxa in bortezomib-induced apoptosis. We found that Noxa protein up-regulation is due to an enhanced transcription of Noxa mRNA. This

last result agrees with the fact that Noxa does not contain PEST sequences and that its high levels could not be only explained by the inhibition of proteasome degradation due to bortezomib (11). Recently, Chen et al. (19) have nicely depicted the high specificity of Noxa for Mcl-1. Moreover, it has been proposed that up-regulated Noxa promotes Bak activation by displacing it from Mcl-1 (11, 18). Consistent with this model, after 18 h of bortezomib treatment, we found a strong association between Mcl-1 and Noxa, whereas Mcl-1/Bak complexes were no more detected. However, the disruption of Mcl-1/Bak complex could be partially due to the observed Bak decrease. We also found free Noxa under bortezomib treatment, indicating that this BH3-only protein may contribute to mitochondria dysfunction by itself as shown previously (24). Furthermore, the exclusive mitochondria location of induced Noxa is compatible with the involvement of this BH3-only protein in mitochondria dysfunction. Of note, we showed for the first time that endogenous Mcl-1/Noxa complexes are present in viable HMCL, suggesting that Noxa is totally kept in check by Mcl-1 as no free Noxa was detected in viable HMCL.

In addition, we have shown previously that in viable myeloma cells, antiapoptotic family members sequester Bim. Among these complexes, we showed that myeloma cell death is totally dependent on Mcl-1/Bim complex disruption (8, 9). In the present study, we found that bortezomib induced an early dissociation of Mcl-1/Bim complexes. Because at the same time point Mcl-1 levels remained constant, we can assume that the high amount of Noxa induced by bortezomib is involved in the displacement of Bim from Mcl-1 binding. According to the fact that Bim belongs to the category of “BH3-only activators,” released Bim could trigger Bax/Bak activation. In this context, the displacement of Bim by Noxa

under bortezomib apoptosis reinforces the model in which the simple inhibition of antiapoptotic molecules is insufficient to induce apoptosis unless a direct BH3-only activator of Bax or Bak is present (25, 26).

Altogether, our results provide a better knowledge of the mechanistic basis for bortezomib sensitivity in multiple myeloma cells. They could also contribute to the design of novel therapeutic interventions like sensitizer BH3 mimetic molecules. Of note, some BH3 mimetic molecules are currently in preclinical development (27).

Acknowledgments

Received 11/27/2006; revised 2/22/2007; accepted 3/21/2007.

Grant support: The Ligue Nationale contre le Cancer (équipe labélisée 2005). S. Wuilleme-Toumi is a recipient of a fellowship from The Association pour la Recherche sur le Cancer.

The costs of publication of this article were defrayed in part by the payment of page charges. This article must therefore be hereby marked *advertisement* in accordance with 18 U.S.C. Section 1734 solely to indicate this fact.

We thank Dr. Lisa Oliver for sharing her expertise in caspases activity assays and Dr. Catherine Gratas and Dr. François Pedelaborde for their advice on real-time quantitative PCR.

References

- Adams J. The development of proteasome inhibitors as anticancer drugs. *Cancer Cell* 2004;5:417–21.
- Richardson PG, Mitsiades C, Hideshima T, Anderson KC. Bortezomib: proteasome inhibition as an effective anticancer therapy. *Annu Rev Med* 2006;57:33–47.
- Cavo M. Proteasome inhibitor bortezomib for the treatment of multiple myeloma. *Leukemia* 2006;20:1341–52.
- Nencioni A, Hua F, Dillon CP, et al. Evidence for a protective role of Mcl-1 in proteasome inhibitor-induced apoptosis. *Blood* 2005;105:3255–62.
- Michels J, Johnson PW, Packham G. Mcl-1. *Int J Biochem Cell Biol* 2005;37:267–71.
- Derenne S, Monia B, Dean NM, et al. Antisense strategy shows that Mcl-1 rather than Bcl-2 or Bcl-x(L) is an essential survival protein of human myeloma cells. *Blood* 2002;100:194–9.
- Gojo I, Zhang B, Fenton RG. The cyclin-dependent kinase inhibitor flavopiridol induces apoptosis in multiple myeloma cells through transcriptional repression and down-regulation of Mcl-1. *Clin Cancer Res* 2002;8:3527–38.
- Gomez-Bougie P, Bataille R, Amiot M. The imbalance between Bim and Mcl-1 expression controls the survival of human myeloma cells. *Eur J Immunol* 2004;34:3156–64.
- Gomez-Bougie P, Oliver L, Le Gouill S, Bataille R, Amiot M. Melphalan-induced apoptosis in multiple myeloma cells is associated with a cleavage of Mcl-1 and Bim and a decrease in the Mcl-1/Bim complex. *Oncogene* 2005;24:8076–9.
- Qin JZ, Ziffra J, Stennett L, et al. Proteasome inhibitors trigger NOXA-mediated apoptosis in melanoma and myeloma cells. *Cancer Res* 2005;65:6282–93.
- Perez-Galan P, Roue G, Villamor N, Montserrat E, Campo E, Colomer D. The proteasome inhibitor bortezomib induces apoptosis in mantle-cell lymphoma through generation of ROS and Noxa activation independent of p53 status. *Blood* 2006;107:257–64.
- Zhu H, Zhang L, Dong F, et al. Bik/NBK accumulation correlates with apoptosis-induction by bortezomib (PS-341, Velcade) and other proteasome inhibitors. *Oncogene* 2005;24:4993–9.
- Descamps G, Wuilleme-Toumi S, Trichet V, et al. CD45neg but not CD45pos human myeloma cells are sensitive to the inhibition of IGF-1 signaling by a murine anti-IGF-1R monoclonal antibody, mAVE1642. *J Immunol* 2006;177:4218–23.
- Smit LA, Hallaert DY, Spijker R, et al. Differential Noxa/Mcl-1 balance in peripheral versus lymph node chronic lymphocytic leukemia cells correlates with survival capacity. *Blood* 2007;109:1660–8.
- Juin P, Pelletier M, Oliver L, et al. Induction of a caspase-3-like activity by calcium in normal cytosolic extracts triggers nuclear apoptosis in a cell-free system. *J Biol Chem* 1998;273:17559–64.
- Gomez-Bougie P, Bataille R, Amiot M. Endogenous association of Bim BH3-only protein with Mcl-1, Bcl-xL, and Bcl-2 on mitochondria in human B cells. *Eur J Immunol* 2005;35:971–6.
- Pfaffl MW. A new mathematical model for relative quantification in real-time RT-PCR. *Nucleic Acids Res* 2001;29:e45.
- Willis SN, Chen L, Dewson G, et al. Proapoptotic Bak is sequestered by Mcl-1 and Bcl-xL, but not Bcl-2, until displaced by BH3-only proteins. *Genes Dev* 2005;19:1294–305.
- Chen L, Willis SN, Wei A, et al. Differential targeting of prosurvival Bcl-2 proteins by their BH3-only ligands allows complementary apoptotic function. *Mol Cell* 2005;17:393–403.
- Voorhees PM, Orłowski RZ. The proteasome and proteasome inhibitors in cancer therapy. *Annu Rev Pharmacol Toxicol* 2006;46:189–213.
- Nijhawan D, Fang M, Traer E, et al. Elimination of Mcl-1 is required for the initiation of apoptosis following ultraviolet irradiation. *Genes Dev* 2003;17:1475–86.
- Han J, Goldstein LA, Gastman BR, Rabinowich H. Interrelated roles for Mcl-1 and BIM in regulation of TRAIL-mediated mitochondrial apoptosis. *J Biol Chem* 2006;281:10153–63.
- Qin JZ, Xin H, Sitailo LA, Denning MF, Nickoloff BJ. Enhanced killing of melanoma cells by simultaneously targeting Mcl-1 and NOXA. *Cancer Res* 2006;66:9636–45.
- Seo YW, Shin JN, Ko KH, et al. The molecular mechanism of Noxa-induced mitochondrial dysfunction in p53-mediated cell death. *J Biol Chem* 2003;278:48292–9.
- Kuwana T, Bouchier-Hayes L, Chipuk JE, et al. BH3 domains of BH3-only proteins differentially regulate Bax-mediated mitochondrial membrane permeabilization both directly and indirectly. *Mol Cell* 2005;17:525–35.
- Certo M, Del Gaizo Moore V, Nishino M, et al. Mitochondria primed by death signals determine cellular addiction to antiapoptotic BCL-2 family members. *Cancer Cell* 2006;9:351–65.
- Reed JC, Pellecchia M. Apoptosis-based therapies for hematologic malignancies. *Blood* 2005;106:408–18.

Cancer Research

The Journal of Cancer Research (1916–1930) | The American Journal of Cancer (1931–1940)

Noxa Up-regulation and Mcl-1 Cleavage Are Associated to Apoptosis Induction by Bortezomib in Multiple Myeloma

Patricia Gomez-Bougie, Soraya Wuillème-Toumi, Emmanuelle Ménoret, et al.

Cancer Res 2007;67:5418-5424.

Updated version Access the most recent version of this article at:
<http://cancerres.aacrjournals.org/content/67/11/5418>

Cited articles This article cites 27 articles, 14 of which you can access for free at:
<http://cancerres.aacrjournals.org/content/67/11/5418.full#ref-list-1>

Citing articles This article has been cited by 48 HighWire-hosted articles. Access the articles at:
<http://cancerres.aacrjournals.org/content/67/11/5418.full#related-urls>

E-mail alerts [Sign up to receive free email-alerts](#) related to this article or journal.

Reprints and Subscriptions To order reprints of this article or to subscribe to the journal, contact the AACR Publications Department at pubs@aacr.org.

Permissions To request permission to re-use all or part of this article, use this link
<http://cancerres.aacrjournals.org/content/67/11/5418>.
Click on "Request Permissions" which will take you to the Copyright Clearance Center's (CCC) Rightslink site.